

Factors Influencing the Reversion of Stress-induced Martensite to Austenite in a Fe-Mn-Si-Cr-Ni Shape Memory Alloy

Leandru G. Bujoreanu, Sergiu Stanciu, Radu I. Comaneci, Markus Meyer, Vasile Dia, and Ciprian Lohan

(Submitted September 2, 2008; in revised form April 16, 2009)

It is well known that one way shape memory effect (SME) in Fe-Mn-Si-based shape memory alloys (SMAs) is related to the thermally induced reversion of ϵ (hexagonal close packed, hcp) stress-induced martensite (SIM) to γ (face centered cubic, fcc) austenite. In the case of a Fe-Mn-Si-Cr-Ni SMA, this reverse martensitic transformation was analyzed in regard to the critical temperature for the beginning of austenite formation (A_s) in different states characterized by quenching temperature and permanent tensile strain. For this purpose, dynamic mechanical analysis (DMA), dilatometry (DIL), differential thermal analysis (DSC), and optical microscopy (OM) were employed to determine the influence of quenching temperature and permanent tensile straining on SIM reversion to austenite during heating.

Keywords critical transformation temperature, Fe-Mn-Si base shape memory alloys, martensite reversion to austenite, stress-induced martensite, thermomechanical and thermodynamic response

1. Introduction

The development of most successful ferrous shape memory alloys (SMAs), based on the Fe-Mn-Si system discovered in Japan at the beginning of 1980's (Ref 1), started with the obtainment of one-way shape memory effect (SME) with recovery degree larger than 97% in Fe-30 Mn-1 Si (hereafter, all the chemical compositions are in mass%) single crystals (Ref 2, 3). Afterward, Murakami et al. first reported that almost 100% SME can be obtained in polycrystalline Fe-30 Mn-6 Si SMAs (Ref 4), then extended composition range to Fe-(28-34) Mn-(4-6) Si (Ref 5) and observed an increased recoverable strain to 4%, by employing thermomechanical training comprising pre-straining and heat treatment (Ref 6). By maintaining silicon content in the range of 5-6% to obtain a good SME, and by adding Cr and Ni to increase corrosion resistance (Ref 7), two potential candidates for low-cost (as compared to NiTi base

alloys) SMA applications were developed: Fe-28 Mn-6 Si-5 Cr and Fe-14 Mn-5 Si-9 Cr-5 Ni (Ref 8).

For a comprehensive characterization of these alloys that undergo a γ (face-centered cubic: fcc) \Leftrightarrow ϵ (hexagonal close-packed: hcp) martensitic transformation (Ref 9), several shape memory phenomena were investigated such as pseudoelastic effect (PSE) (Ref 10, 11) and “apparent” two-way shape memory effect (TWSME) which was revealed (Ref 12) after suitable training (Ref 13). A mechanism of reversible stress-induced transformation, from tension-induced to compression-induced ϵ martensite, was proposed (Ref 14).

However, the SME, related to the thermally induced reversion of ϵ stress-induced martensite (SIM) to γ austenite, accompanied by recoverable strains of about 5%, has presently remained the most prominent characteristic of the Fe-Mn-Si SMAs (Ref 15) which are able to develop recovery stresses as high as 500 MPa (Ref 16) by tensile-constrained recovery (Ref 17).

In the particular case of corrosion-resistant Fe-Mn-Si-Cr-Ni SMAs, intensive research was carried out on the ϵ SIM regarding its growth (Ref 18) and preferred formation due to the occurrence (Ref 19) and alignment (Ref 20) of second-phase precipitates, as well as on the influence of variant intersections on the transformation behavior (Ref 21) and on the reversibility-assistance by back-stress developed at martensite-band tips (Ref 22). The basic conclusion that has been drawn is that ϵ SIM plates should be as narrow as possible, with a single variant orientation and should interact neither with each other nor with thermally induced martensite (Ref 23).

Among the factors that might influence ϵ SIM reversion on heating, the annealing temperature and the amount of pre-strain were analyzed in the case of Fe-13 Mn-5 Si-(9-10) Cr-(6-7) Ni SMAs. The results showed that in Fe-13 Mn-5 Si-10 Cr-6 Ni alloy (Ref 24) the start temperature, A_s , for martensite reversion, on heating, tends to decrease with increasing annealing temperature while it remains almost constant with increasing pre-strain. On the other hand, in Fe-13 Mn-5 Si-9

This article is an invited paper selected from presentations at Shape Memory and Superelastic Technologies 2008, held September 21-25, 2008, in Stresa, Italy, and has been expanded from the original presentation.

Leandru G. Bujoreanu, Sergiu Stanciu, Radu I. Comaneci, and Ciprian Lohan, Faculty of Materials Science and Engineering, The “Gheorghe Asachi” Technical University from Iasi, Bd. D. Mangeron 61A, Iasi 700050, Romania; **Markus Meyer**, BU Analyzing & Testing, NETZSCH, Gerätebau GmbH, Wittelsbacherstrasse 42, 95100 Selb, Bavaria, Germany; and **Vasile Dia**, Laboratory Department, ARCELOR MITTAL Tubular Products Iasi, Calea Chişinăului 132, Iasi 700180, Romania. Contact e-mail: lgbujo@tuiasi.ro.

Cr-7 Ni alloy (Ref 25), the magnitude of shape recovery augmented with increasing annealing temperature from 870 K to 1070 K and cold rolling up to 15%.

The presence of carbon, limited to a maximum value of 0.3%, has been considered to be beneficial for Fe-Mn-Si-Cr-Ni SMAs since it contributes to the reinforcement of the austenite (Ref 26).

This article aims to bring additional evidence on the influence of both the temperatures of the heat treatment and the pre-straining on the start temperature A_s for ϵ SIM reversion, on heating, in the case of a Fe-Mn-Si-Cr-Ni SMA with high carbon content.

2. Experimental Procedure

From a Fe-Mn-Si-Cr-Ni SMA which was cast, homogenized (1270 K, 5×3.6 ks, water), and hot rolled (1270 K), specimens were cut with gauge dimensions $1 \times 5 \times 10 \times 10^{-3}$ m. The chemical composition was determined by spectrogravimetry as 13.9 Mn, 6.3 Si, 3.34 Cr, 1.61 Ni, 0.6 C, 0.12 Cu, 0.1 P, 0.05 S, and balance Fe. The specimens were analyzed in 12 different states characterized by three different heat treatments (Q_{1-3}) in each of which the formation of ϵ SIM, as compared to initial state E_0 , was expected to occur as an effect of applying three different nominal permanent elongations (E_{1-3}), by means of an INSTRON 3382 tensile testing machine at room temperature (RT). Owing to uncontrollable spring back during unloading, a tolerance of $\pm 0.05\%$ was considered as compared to the nominal values of permanent strain listed in Table 1. Accordingly, the 12 states were designated as $Q_i E_j$, where $i = 1, 2, 3$ and $j = 0, 1, 2, 3$; for instance, state $Q_2 E_3$ refers to specimens quenched from 1320 K with permanent pre-strains ranging from 2.05% to 2.15%. In each of the above 12 states, three specimens were prepared for dynamic mechanical analyzer (DMA) and three for dilatometer (DIL).

In order to determine the influence of quenching temperature and permanent elongation on thermally induced reversion of martensite to austenite, both thermomechanical and thermodynamic responses of Fe-Mn-Si-Cr-Ni SMA were evaluated during heating.

Thermomechanical response was examined by means of a DMA and a DIL. Three DMA experiments were conducted, on specimens belonging to each of the above 12 states, on a NETZSCH DMA 242 device, functioning in 3 point bending mode, also called forced 3 point beam mode (Ref 27), at a frequency of 1 Hz and an amplitude of 20×10^{-6} m. Heating was performed at a rate of 5×10^{-2} K/s from RT to 620 K. Based on specimen dimensions, and on the force and displacement signals, both internal friction ($\tan \Phi$) and elastic

Table 1 Designation of the 12 heat-treated specimens of Fe-Mn-Si-Cr-Ni SMA analyzed in initial and permanently elongated states

State	Quenching temperature, K	Q_1 1270	Q_2 1320	Q_3 1370
E_0	Nominal permanent strain, %	0	0	0
E_1		1.1	1.4	1.9
E_2		1.5	1.7	2.15
E_3		1.9	2.1	2.5

modulus (E) were evaluated during heating. DIL measurements were performed on a NETZSCH DIL 402 CD dilatometer, at a heating rate of 8.33×10^{-2} K/s up to 870 K, under He atmosphere. Fused silica and alumina were used as sample holder material and standard calibration material, respectively. In this case, as well, three measurements were performed on each state of the specimens. For DIL evaluation, the variations with temperature of the relative elongation (dL/L_0), expansion rate $d(dL/L_0)/dt$, and thermal expansion coefficient (α) were analyzed.

Thermodynamic response was recorded by a NETZSCH STA 449 F3 device during a heating-cooling cycle between RT and 870 K, under Ar atmosphere, at a rate of 1.66×10^{-1} K/s.

In order to reveal the formation of ϵ SIM under an applied nominal permanent elongation, optical micrographs were recorded on fragments cut from the deformed gauge of the elongated specimens, which were embedded into resin, electro polished, and etched with 10% Nital solution before being analyzed on a NEOPHOT 32 optical microscope.

3. Results and Discussions

Two typical examples of DMA results recorded on specimens quenched from 1320 K are illustrated in Fig. 1. It is known that, at low frequency such as 1 Hz, a high internal friction peak ($\tan \Phi$) (Ref 28) and a step-like modulus (E) variation (Ref 29) are associated with the hcp \rightarrow fcc transition, in the case of low-manganese Fe-Mn-Si-based SMAs (Ref 30). This evolution is observed in Fig. 1(a) corresponding to an unstrained specimen which was quenched from 1320 K. $\tan \Phi$ peak exceeds 0.02 and E increases with approx. 3.7 GPa during heating, which suggests that a solid state transition, such as reverse martensitic transformation, could be responsible for these changes. As an effect of pre-straining, multiple peaks were noticeable in most of the cases, in the variation of $\tan \Phi$ with temperature, such as that shown in Fig. 1(b), which corresponds to a specimen pre-strained with 2.07%. This rather erratic behavior, in the variation of $\tan \Phi$ with temperature could be an effect of specimen shrinkage, due to SME triggering, since the specimens tend to recover their unstrained shape on heating, or could be an effect of multiple stages of the martensite reversion. On the other hand, it has been shown that the change in the temperature coefficient, occurring on the modulus curve, is related to shape recovery of the specimen during heating since “modulus softening” is associated with the reverse $\epsilon \rightarrow \gamma$ transformation (Ref 31). Therefore, in those cases where it was possible, A_s was evaluated as the point where modulus increase on heating started for the first time (Ref 32). The determined values of A_s are summarized in Table 2. As known from Table 1, permanent elongation increases from Q_{i1} to Q_{i3} which suggests that the SIM amount also increases in the same way. On the other hand, it is known that $\tan \Phi$ is increased by SIM formation (Ref 33) and, for this reason, the highest value, of 0.033, was reached in state $Q_3 E_3$, which corresponds to the largest permanent elongation of 2.53%. From an analysis of the A_s values listed in Table 2, we can notice that A_s tends to decrease with increasing permanent applied strain, within the quenched states, Q_2 and Q_3 . Therefore, from the point of view of thermomechanical response on heating, as determined by DMA, it may be estimated that the critical start temperature for SIM reversion

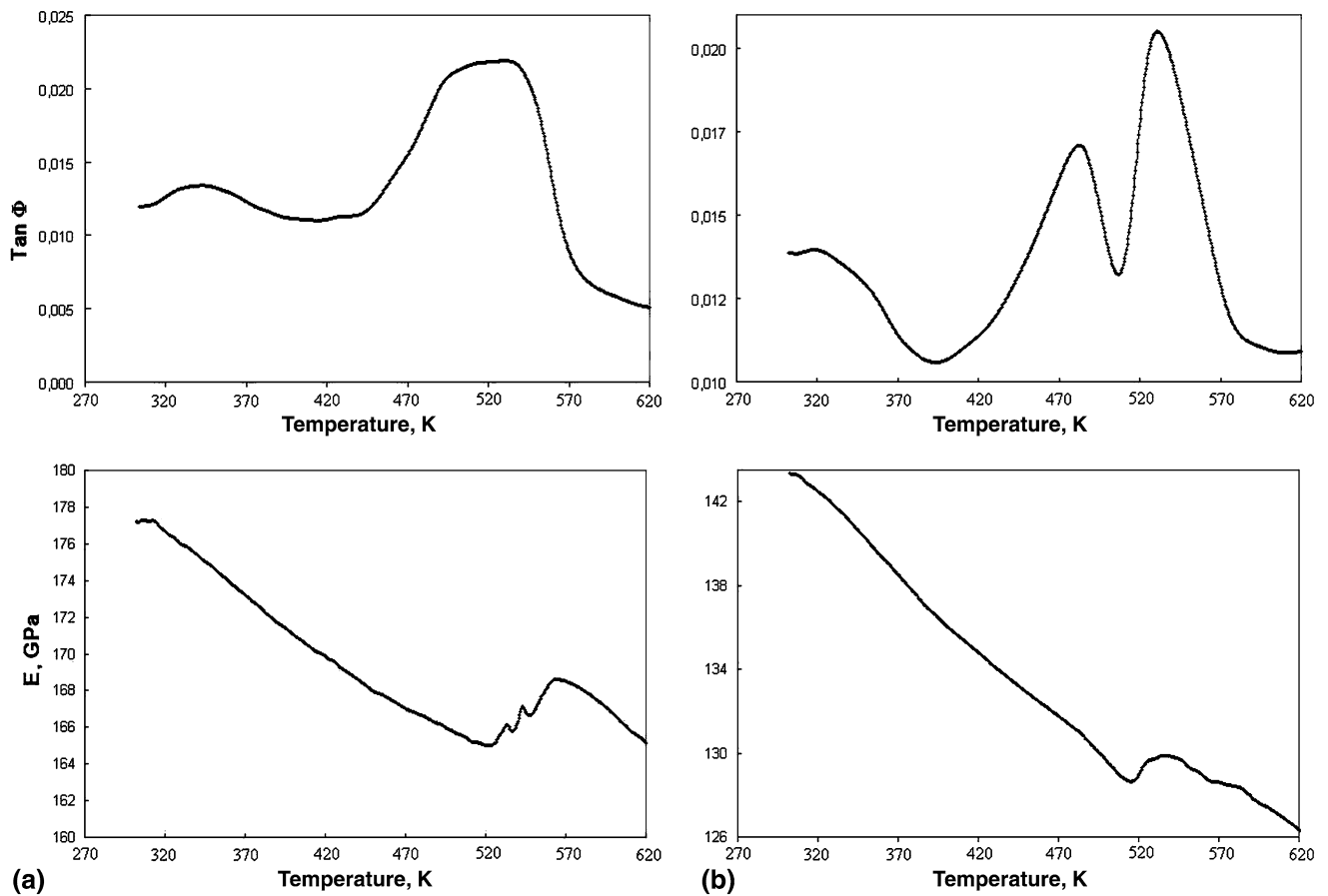


Fig. 1 Variations of internal friction ($\text{Tan } \Phi$) and elastic modulus (E) determined by DMA measurements in 3 point bending mode, with a frequency of 1 Hz and an amplitude of 20×10^{-6} m, during heating to 620 K of the specimens of Fe-Mn-Si-Cr-Ni SMA under study, quenched from 1320 K (Table 1): (a) Q_2E_0 ; (b) Q_2E_3

Table 2 Values of critical transformation temperatures for martensite reversion start on heating, estimated from DMA experiments

	Heat treatment state											
	Q_1				Q_2				Q_3			
	E_0	E_1	E_2	E_3	E_0	E_1	E_2	E_3	E_0	E_1	E_2	E_3
Permanent elongation state:	...	553	522	510	502	506	...	498	485	477
A_s , K	...	553	522	510	502	506	...	498	485	477

to austenite tends to decrease with increasing permanent elongation.

The second evaluation, aiming to reveal the effects of both quenching temperature and pre-straining on thermomechanical response of Fe-Mn-Si-Cr-Ni SMA under study, was performed by dilatometry which enables accurate monitoring of relative elongation (dL/L_0), expansion rate $d(dL/L_0)/dt$, and thermal expansion coefficient (α) due to temperature variation on heating. The effect of quenching temperature on unstrained specimens is illustrated in Fig. 2. Since the specimens were not deformed, they should not contain any SIM. Consequently no obvious inflections were noticeable on the dilatograms, in spite of the amount of thermally induced martensite which is expected to exist, according to DMA results shown in Fig. 1(a). Moreover, we can notice that both expansion rate $d(dL/L_0)/dt$ and thermal expansion coefficient (α) varied in the same way in

the three quenching states, during heating, although α seemed to decrease with increasing quenching temperature. On the other hand, with increasing quenching temperature, an increase of the amount of thermally induced martensite is expected to occur as indicated by Fig. 1(a) and by the variations of tensile mechanical characteristics listed in Table 3. As a matter of fact, the ultimate tensile stress decreased and the ultimate strain exhibited a tendency to increase, so it may be assumed that the specimens became more ductile with increasing quenching temperature. The only transformation (confirmed by the sharp decrease of $d(dL/L_0)/dt$ is located at around 830 K in Fig. 2(b), corresponding to Q_2E_0 state (1320 K) and probably also to Q_3E_0 (although heating was stopped at 770 K). It is assumed that this inflection could correspond to the transformation of stabilized thermally induced martensite to bainite (Ref 34). The effect of permanent elongation on the thermomechanical

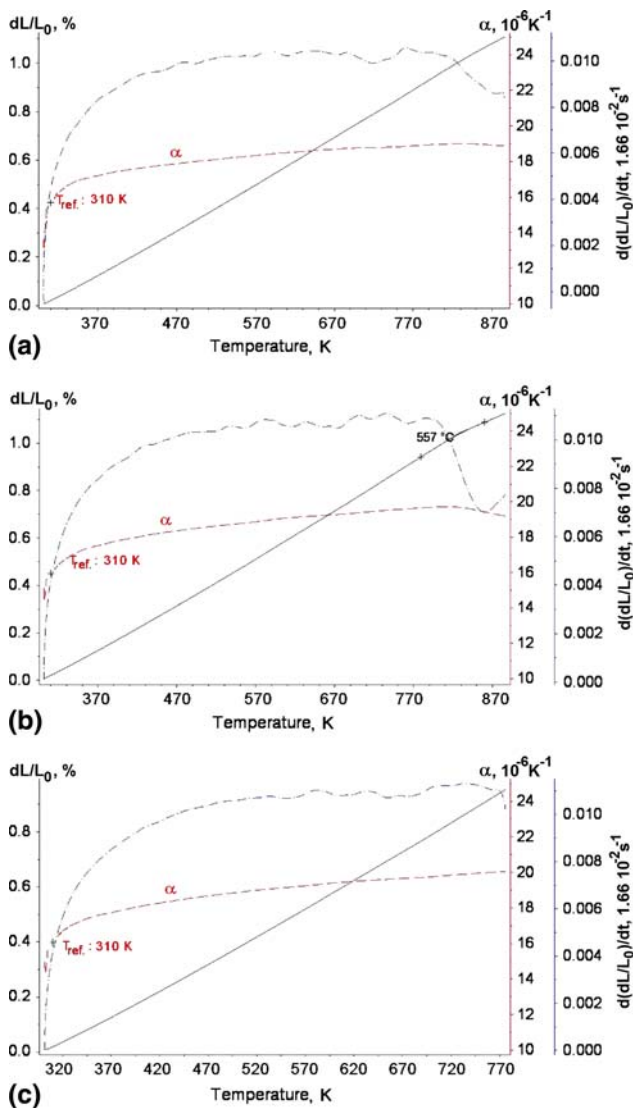


Fig. 2 Variations with temperature of relative elongation (dL/L_0 with solid line), expansion rate $d(dL/L_0)/dt$, and thermal expansion coefficient (α), on the dilatograms recorded during the heating of unstrained specimens of Fe-Mn-Si-Cr-Ni SMA under study, in different heat-treated states (Table 1): (a) Q_1E_0 ; (b) Q_2E_0 ; (c) Q_3E_0

Table 3 Values of mechanical parameters determined by tensile tests

Heat treatment state	Q_1	Q_2	Q_3
Ultimate stress, MPa	523	395	373
Ultimate strain, %	4.68	14.88	11.48

response of the specimens quenched from 1270 K is illustrated in Fig. 3. It is obvious that, with increasing nominal permanent elongation from 1.1 to 1.9, a solid-state transition becomes more and more evident. Therefore, from the point of view of thermomechanical response determined by dilatometry during heating, it may be assumed that the amount of SIM has been very low so that it is only at high permanent elongations, such as in specimen Q_1E_3 , where SIM reversion to austenite could be

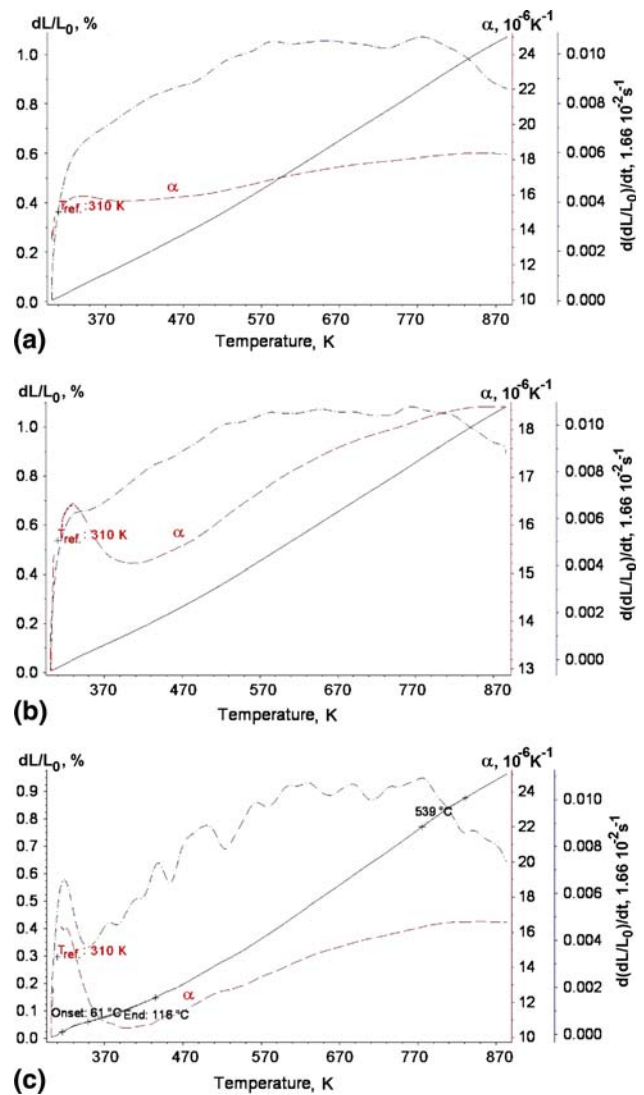


Fig. 3 Variations with temperature of relative elongation (dL/L_0 with solid line), expansion rate $d(dL/L_0)/dt$, and thermal expansion coefficient (α), on the dilatograms recorded during the heating of specimens of Fe-Mn-Si-Cr-Ni SMA under study, in heat-treated state Q_1 in different permanently elongated states (Table 1): (a) Q_1E_1 ; (b) Q_1E_2 ; (c) Q_1E_3

detected. In Fig. 3(c), corresponding to state Q_1E_3 , the start temperature of the transition is about 331 K. This transition is accompanied by marked fluctuations of $d(dL/L_0)/dt$ and (α), and the entire aspect of the dilatogram is very similar to that found in literature (Ref 35).

The thermodynamic response is illustrated in Fig. 4 by the DSC versus temperature diagram of a fragment cut from the elongated gauge of Q_1E_3 specimen. It is assumed that the first shallow endothermic peak could fairly correspond to SIM reversion to austenite. This is suggested for two reasons: (i) it starts at around 370 K which is close to the value $A_s = 331$ K determined by dilatometry studies and (ii) it has a flat and not a sharp minimum since it was generated by a small fragment of the elongated gauge which could incorporate very small amounts of SIM. The second endothermic peak shows that an obvious transition occurred during heating, between 663 and 822 K, which is close to 830 K, the value presumed to

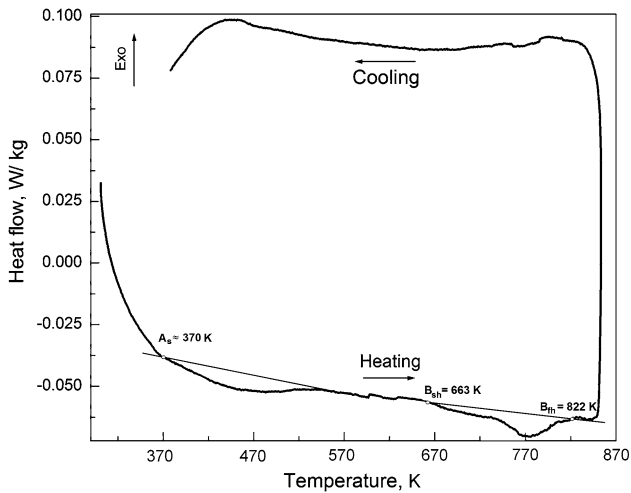


Fig. 4 DSC thermogram, recorded during a heating-cooling cycle between room temperature and 870 K, indicating a reversible martensitic transformation in a fragment cut from the elongated gauge of a specimen of Fe-Mn-Si-Cr-Ni SMA under study in state Q_1E_3

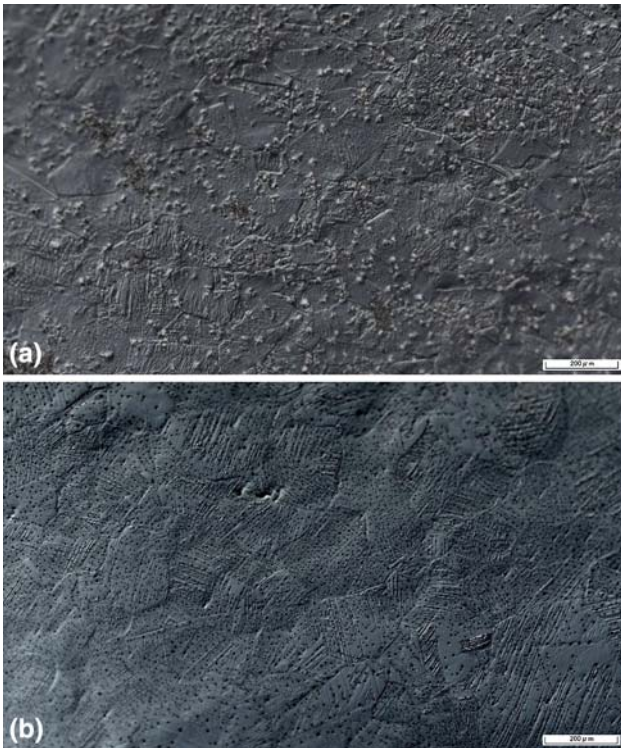


Fig. 5 OM micrographs of specimens of Fe-Mn-Si-Cr-Ni SMA under study, quenched from 1270 K: (a) unstrained, Q_1E_0 ; (b) pre-strained 1.9%, Q_1E_3

correspond to the transformation of stabilized thermally induced martensite to bainite, as determined by dilatometry.

Finally, two optical micrographs are shown in Fig. 5 for the states Q_1E_0 and Q_1E_3 , respectively. Figure 5(a) reveals that after 1270 K-quenching, scarce thermally induced ϵ martensite plates are noticeable on some of the grains, while Fig. 5(b) shows that, as an effect of applying 1.9% permanent elongation, the plates became significantly denser and finer.

4. Summary and Conclusions

A Fe-13.9 Mn-6.3 Si-3.34 Cr-1.61 Ni-0.6 C SMA was subjected to three different quenching temperatures (1270, 1320, and 1370 K, respectively) and three permanent elongations (between 1.1% and 2.5%), for each of the quenched states, to stress induce ϵ martensite. Martensite reversion to austenite during heating was evaluated by means of thermomechanical and thermodynamic responses. The former response was determined by DMA and dilatometry and the latter by STA.

Owing to the low amount of stress-induced martensite and to the different sensitivities of the three techniques, different aspects were revealed by each experimental investigation:

- (i) DMA recorded multiple $\tan \Phi$ peaks, reaching values as high as 0.033, suggesting a multiple-stage reversion of stress-induced martensite to austenite during heating. A_s values, estimated by DMA and corresponding to the point where elastic modulus increase occurred on heating, for the first time, tend to slightly increase with increasing quenching temperature and to decrease with increasing permanent elongation;
- (ii) Dilatometry revealed reversion of the stress-induced martensite to austenite and the formation of increasingly larger amounts of thermally induced martensite, which was found to transform to recovery bainite at around 830 K;
- (iii) STA data showed that the reversion of the stress-induced martensite to austenite absorbs much lower specific energy as compared to the transition of stabilized thermally induced martensite to recovery bainite;
- (iv) The existence of thermally induced martensite in quenched state and of stress-induced martensite in pre-strained state was ascertained by optical microscopy.

Acknowledgments

This study was financially supported by UEFISCU by means of the research Grant PN II-ID 301-PCE-2007-1, Contract no. 279/01.10.2007. Special thanks are due to Dr. Takahiro Sawaguchi, NIMS Tsukuba, for fruitful scientific discussions.

References

1. T. Maki, Ferrous Shape Memory Alloys, *Shape Memory Materials*, K. Otsuka and C.M. Wayman, Ed., Cambridge University Press, Cambridge, 1998, p 117–132
2. A. Sato, E. Chishima, K. Soma, and T. Mori, Shape Memory Effect in $\gamma \leftrightarrow \epsilon$ Transformation in Fe-30Mn-1Si Alloy Single Crystals, *Acta Metall.*, 1982, **30**, p 1177–1183
3. A. Sato, E. Chishima, Y. Yamaji, and T. Mori, Orientation and Composition Dependencies of Shape Memory Effect in Fe-Mn-Si Alloys, *Acta Metall.*, 1984, **32**, p 539–547
4. M. Murakami, H. Suzuki, and Y. Nakamura, Effect of Si on the Shape Memory Effect of Polycrystalline Fe-Mn-Si Alloys, *Trans. ISIJ*, 1987, **27**, p B-87
5. M. Murakami, H. Otsuka, H. Suzuki, and S. Matsuda, Effect of Alloying Content, Phase and Magnetic Transformation on the Shape Memory Effect of Fe-Mn-Si Alloys, *Trans. ISIJ*, 1987, **27**, p B-88
6. M. Murakami, H. Otsuka, and S. Matsuda, Improvement of Shape Memory Effect of Fe-Mn-Si Alloys, *Trans. ISIJ*, 1987, **27**, p B-89

7. H. Otsuka, H. Yamada, T. Maruyama, H. Tanahashi, S. Matsuda, and M. Murakami, Effects of Alloying Additions on Fe-Mn-Si Shape Memory Alloys, *ISIJ Int.*, 1990, **30**, p 674–679
8. S. Kajiwara, Characteristic Features of Shape Memory Effect and Related Transformation Behavior in Fe-Based Alloys, *Mater. Sci. Eng. A*, 1999, **273–275**, p 67–88
9. T.Y. Hsu and X. Zuyao, Martensitic Transformation in Fe-Mn-Si Based Alloys, *Mater. Sci. Eng. A*, 1999, **273–275**, p 494–497
10. O. Matsumura, T. Sumi, N. Tamura, K. Sakao, T. Furukawa, and H. Otsuka, Pseudoelasticity in an Fe-28Mn-6Si-5Cr Shape Memory Alloy, *Mater. Sci. Eng. A*, 2000, **279**, p 201–206
11. T. Sawaguchi, T. Kikuchi, and S. Kajiwara, The Pseudoelastic Behavior of Fe-Mn-Si-based Shape Memory Alloys, Containing Nb and C, *Smart Mater. Struct.*, 2005, **14**, p S317–S322
12. J.H. Yang, H. Chen, and C.M. Wayman, Development of Fe-Based Shape Memory Alloys Associated with Face-Centered Cubic-Hexagonal Close-Packed Martensitic Transformations: Part I. Shape Memory Behavior, *Metall. Trans. A*, 1992, **23A**, p 1431–1437
13. T. Shiming, L. Jinhai, and Y. Shiwei, Two-Way Shape Memory Effect of an Fe-Mn-Si Alloy, *Scripta Metall. Mater.*, 1991, **25**, p 1119–1121
14. T. Sawaguchi, L.G. Bujoreanu, T. Kikuchi, K. Ogawa, M. Koyama, and M. Murakami, Mechanism of Reversible Transformation-Induced Plasticity of Fe-Mn-Si Shape Memory Alloys, *Scripta Mater.*, 2008, **59**, p 826–829
15. N. Stanford, D.P. Dunne, and H. Li, Re-examination of the Effect of NbC Precipitation on Shape Memory in Fe-Mn-Si-Based Alloys, *Scripta Mater.*, 2008, **58**, p 583–586
16. Y. Wen, N. Li, and M. Tu, Effect of Quenching Temperature on Recovery Stress of Fe-18Mn-5Si-8Cr-4Ni Alloy, *Scripta Mater.*, 2001, **44**, p 1113–1116
17. L.G. Bujoreanu, V. Dia, S. Stanciu, M. Susan, and C. Baciuc, Study of the Tensile Constrained-Recovery Behavior of a Fe-Mn-Si Shape Memory Alloy, *Eur. Phys. J. Special Top.*, 2008, **158**, p 15–20
18. J.H. Yang and C.M. Wayman, Self-Accommodation and Shape Memory Mechanism of ϵ -Martensite—I. Experimental Observations, *Mater. Charact.*, 1992, **28**, p 23–35
19. S. Kajiwara, D. Liu, T. Kikuchi, and N. Shinya, Remarkable Improvement of Shape Memory Effect in Fe-Mn-Si Based Shape Memory Alloys by Producing NbC Precipitates, *Scripta Mater.*, 2001, **44**, p 2809–2814
20. Y.H. Wen, W. Zhang, N. Li, H.B. Peng, and L.R. Xiong, Principle and Realization of Improving Shape Memory Effect in Fe-Mn-Si-Cr-Ni Alloy through Aligned Precipitations of Second-Phase Particles, *Acta Mater.*, 2007, **55**, p 6526–6534
21. J.H. Yang, H. Chen, and C.M. Wayman, Development of Fe-Based Shape Memory Alloys Associated with Face-Centered Cubic-Hexagonal Close-Packed Martensitic Transformations: Part II. Transformation Behavior, *Metall. Trans. A*, 1992, **23A**, p 1439–1444
22. N. Bergeon, G. Guenin, and C. Esnouf, Microstructural Analysis of the Stress-induced ϵ Martensite in a Fe-Mn-Si-Cr-Ni Shape Memory Alloy. Part II: Transformation Reversibility, *Mater. Sci. Eng. A*, 1998, **242**, p 87–95
23. Y.H. Wen, N. Li, and L.R. Xiong, Composition Design Principles for Fe-Mn-Si-Cr-Ni Based Alloys with Better Shape Memory Effect and Higher Recovery Stress, *Mater. Sci. Eng. A*, 2005, **407**, p 31–35
24. H. Li, D. Dunne, and N. Kennon, Factors Influencing Shape Memory Effect and Phase Transformation Behaviour of Fe-Mn-Si Based Shape Memory Alloys, *Mater. Sci. Eng. A*, 1999, **273–275**, p 517–523
25. N. Stanford and D.P. Dunne, Thermo-Mechanical Processing and the Shape Memory Effect in an Fe-Mn-Si-Based Shape Memory Alloy, *Mater. Sci. Eng. A*, 2006, **422**, p 352–359
26. L. Chengxin, W. Guixin, W. Yandong, L. Qingsuo, and Z. Jianjun, Effect of Addition of V and C on Strain Recovery Characteristics in Fe-Mn-Si Alloy, *Mater. Sci. Eng. A*, 2006, **438–440**, p 808–811
27. T. Sawaguchi, L.G. Bujoreanu, T. Kikuchi, K. Ogawa, and F. Yin, Effects of Nb and C in Solution and in NbC Form on the Transformation-related Internal Friction of Fe-17 Mn (mass. %) Alloys, *ISIJ Int.*, 2008, **48(1)**, p 99–106
28. J.E. Bidaux, R. Schaller, and W. Benoit, Study of the h.c.p.-f.c.c. Phase Transition in Cobalt by Acoustic Measurements, *Acta Metall.*, 1989, **37**, p 803–811
29. J. Van Humbeeck, J. Stoiber, L. Delaey, and Rolf. Gotthardt, The High Damping Capacity of Shape Memory Alloys, *Z. Metallkd.*, 1995, **86**, p 176–183
30. A.K. De, N. Cabanas, and B.C. De Cooman, Fcc-hcp Transformation-Related Internal Friction in Fe-Mn Alloys, *Z. Metallkd.*, 2002, **93**, p 228–235
31. J.F. Wan, S.P. Chen, T.Y. Hsu, and Y.N. Huang, Modulus Softening during the $\gamma \rightarrow \epsilon$ Martensitic Transformation in Fe-25 Mn-6 Si-5 Cr-0.14 N Alloy, *Mater. Sci. Eng. A*, 2006, **438–440**, p 887–890
32. A. Sato, K. Ozaki, Y. Watanabe, and T. Mori, Internal Friction due to $\epsilon \rightarrow \gamma$ Reverse Transformation in an Fe-Mn-Si-Cr Shape Memory Alloy, *Mater. Sci. Eng. A*, 1988, **101**, p 25–30
33. T. Sawaguchi, T. Kikuchi, F. Yin, and S. Kajiwara, Internal Friction of an Fe-28Mn-6Si-5Cr-0.5NbC Shape Memory Alloy, *Mater. Sci. Eng. A*, 2006, **438–440**, p 796–799
34. H.K.D.H. Bhadeshia, *Bainite in Steels*, 2nd ed., IOM Communications Ltd, London, 2001
35. N. Van Caenegem, L. Duperez, K. Verbeke, D. Segers, and Y. Houbaert, Stress Related to the Shape Memory Effect in Fe-Mn-Si-based Shape Memory Alloys, *Mater. Sci. Eng. A*, 2008, **481–482**, p 183–189